Polymer 50 (2009) 5170–5174

Contents lists available at ScienceDirect

Polymer

journal homepage: www.elsevier.com/locate/polymer

Polymer Communication

Controlled organization of self-assembled rod-coil block copolymer micelles

Yingfeng Tu [a,b], Matthew J. Graham [b], Ryan M. Van Horn [b], Erqian Chen [a], Xinhe Fan [a], Xiaofang Chen [a], Qifeng Zhou [a,*], Xinhua Wan [a,**], Frank W. Harris [b], Stephen Z.D. Cheng [b,***]

[a] *Department of Polymer Science & Engineering, College of Chemistry and Molecular Engineering, Peking University, Beijing 100871, PR China*
[b] *The Maurice Morton Institute and Department of Polymer Science, The University of Akron, Akron, OH 44325, USA*

ARTICLE INFO

Article history:
Received 20 June 2009
Received in revised form
28 August 2009
Accepted 2 September 2009
Available online 6 September 2009

Keywords:
Rod-coil block copolymers
Self-assembly
Micelles

ABSTRACT

Spherical micelles of a series of poly(styrene-*block*-(2,5-bis[4-methoxyphenyl]oxycarbonyl)styrene) (PS-*b*-PMPCS) rod-coil diblock copolymers in a selective solvent can organize into large mono-layered films with a well-ordered hexagonal packing of the spheres after solvent evaporation. Organized domains in the spherical micelle film were observed by transmission electron microscopy (TEM) and atomic force microscopy (AFM). The core-shell structure of the spherical micelle remained after solvent evaporation. The micelle diameter in the ordered film as observed by TEM and AFM agree. The size of the spherical micelles can be controlled by the length of PMPCS when the length of the PS is fixed. The sphere diameters were varied from several tens of nanometers to more than one hundred nanometers. Solutions of smaller micelle spheres formed less ordered films than those from larger micelle particles. Additionally, monolayer films of cylindrical worm-like micelles were also prepared. Those cylindrical micelles were observed to be end-capped by spherical micelles. The monolayer micelle film from the largest spherical micelles appeared red when observed in optical microscopy in the reflection mode. A broad adsorption peak with a maximum adsorption wavelength of 545 nm was observed *via* UV–Vis spectroscopy.

1. Introduction

Block copolymers have attracted increasing attention as a promising means to form a variety of periodic patterns at the nanometer scale due to their self-assembly with the nanodomain properties being controlled by the block copolymer's various physical and chemical properties and domain sizes and morphologies being controlled by the block copolymer composition and volume fraction [1–5]. Solvent annealing can enhance the block copolymers' self-assembly in bulk to give better orientation and lateral ordering of the nanodomains with domain sizes ranging from 5 nm to 100 nm [6–11]. In selective solvents, block copolymers can self-assemble to form polymeric micelles. The morphology of these micelles ranges among spherical micelles, rods, vesicles, compound micelles, lamellae, nano-ribbons, disk-like aggregates and mushroom-like structures with sizes ranging from a few nanometers to microns [12–20]. In addition to the ability to form monodisperse micelles on the appropriate length scale, block copolymers allow one to precisely tailor the interactions between micelles which can help direct supramolecular self-assembly [21,22].

The ability to use self-assembled block copolymer micelles to generate functionalized ordered structures on the nanoscale has attracted much less attention compared to bulk copolymer [23–37]. Möller and coworkers used the self-assembly of polystyrene-*b*-poly(2-vinylpyridine) diblock copolymer micelles to form uniform monolayer films [25]. By loading the micelles with gold ions, which were later reduced to gold nanoparticles, they produced well-organized gold dots with a diameter of a few nanometers and a spacing of several tens of nanometers. Kronholz et al. used the same template to produce $PbTiO_3$ nano-grains with a diameter of 30 nm without using time-consuming and expensive e-beam lithography [33]. However, in both of these efforts, the micelle films were not very uniform because the micelle size was not easy to control. In addition, the loading of gold particles is limited because neither the swollen outside shell of the micelles, which shrank during micelle film formation, nor the core can contain a large quantity of metal. To obtain well-ordered, controlled nanodomains from block copolymer micelles, the micelle system must fulfill the following requirements: the micelle morphology needs to be very uniform and fixed during the solvent evaporation process; the

---

[*] Corresponding author. Tel.: +86 10 6275 1726.
[**] Corresponding author. Tel.: +86 10 6275 4187.
[***] Corresponding author. Tel.: +1 330 972 6931.
E-mail addresses: qfzhou@pku.edu.cn (X. Zhou), xhwan@pku.edu.cn (X. Wan), scheng@uakron.edu (S.Z.D. Cheng).

0032-3861/$ – see front matter © 2009 Elsevier Ltd. All rights reserved.
doi:10.1016/j.polymer.2009.09.006

micelle size and morphology should be controlled by the block copolymer length and/or copolymer concentration; and the critical micelle concentration (CMC) should be low enough that polymer unimers in the film can be neglected. To meet these requirements, a single solvent system with one long insoluble block is preferred.

We have reported that poly(styrene-*block*-(2,5-bis[4-methoxyphenyl]oxycarbonyl)-styrene) (PS-*b*-PMPCS) block copolymers can self-assemble in *p*-xylene to form spherical micelles under most conditions [38,39]. The micelle spherical core diameter was controlled by the PMPCS block length when the PS length was fixed. At some concentrations, cylindrical micelles were observed. The CMC of the block copolymer was very low and could be ignored when the PMPCS block length was long. The micelles formed when cooling the solution from high temperature (120 °C) to room temperature, and the morphology was fixed independent of any changes in concentration after cooling. These characteristics enable this diblock copolymer system to be an ideal model to test the assembly of block copolymer micelles for possible optical applications.

In this paper, we prepared well-ordered, hexagonal close packed monolayer micelle films from PS-*b*-PMPCS block copolymer micelles in *p*-xylene by evaporating the solvent on the surface of water. The monolayer allows us to examine the size distribution of the micelles, packing quality, and defect levels without the effect of defect build-up through many layers. Transmission electron microscopy (TEM) and atomic force microscopy (AFM) results were consistent concerning the size of the micelles comprising the film. To demonstrate control over the micelle size, block copolymers with different PMPCS block lengths were synthesized, and the size of the micelle diameters predictably ranged from 30 nm to 140 nm. The film with the largest micelles had a reflection band (optical stop-band) at about 540 nm and appeared red under ambient light conditions. Cylindrical micelles can also form monolayer micelle films but had many defects.

2. Experimental section

2.1. Sample preparation

The synthesis of the block copolymers has been reported elsewhere [40]. PS-TEMPO was used as the macro-initiator and had a number average molecular weight of 64,600 Da with a polydispersity of 1.20 obtained by comparison to the molecular weight calibration curve from linear PS standards. The molecular weight of PMPCS was calculated from ^{1}H NMR using CD_2Cl_2 as the solvent by estimating the ratio of peak areas for the methoxy groups (3.3–3.8) to aromatic groups (6.3–7.2). To test if the micelle size and shape can be tuned by block copolymer length, five block copolymers with the same PS length and different PMPCS lengths were synthesized as indicated in Fig. 1.

The micelle solutions were prepared with concentrations of 2.0 mg/ml. The block copolymer was put into *p*-xylene and heated to 120 °C for 12 h then quenched to room temperature. These were used as a stock solution and diluted for lower concentration solutions. Then, the dilute solutions were exposed to the same heating and quenching processes. For spherical micelle monolayer formation, micelle films were formed by casting 20 µl of block copolymer solution in *p*-xylene with a concentration of 2.0 mg/ml onto a circular water surface with an area of 7 cm^2. For cylindrical micelles, the film was obtained by casting 100 µl of block copolymer solution in *p*-xylene with a concentration of 0.06 mg/ml onto a 7 cm^2 water surface area. When *p*-xylene evaporated (or dissolved slowly into water), the organic layer shrank to minimize surface energy. For TEM observation, films were transferred to carbon-coated copper grids. For AFM and optical microscopy, films were transferred to clean glass slides. Samples were put into a vacuum oven for 1 day to remove the residual solvent and water.

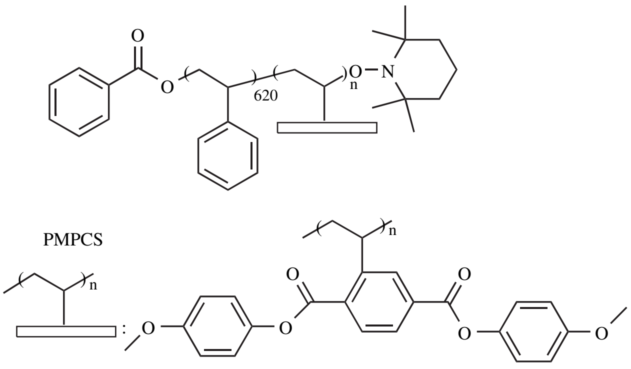

Copolymer	Repeating Units of MPCS^a	Polydispersity^b
1	1890	1.37
2	1000	1.35
3	310	1.25
4	180	1.24

a: Measured by NMR.
b: Measured by SEC.

Fig. 1. Chemical structure and polydispersity of the synthesized PS-*b*-PMPCS block copolymers.

2.2. Equipment

TEM experiments were performed on a JEM-100CX II transmission electron microscope at an accelerating voltage of 120 kV; samples were observed without staining. A Nanoscope IIIA AFM (Digital Instruments/Veeco Metrology Group) in tapping mode was used to observe the film surface morphology with a typical scan size of 5 µm, a scan rate of 1 Hz, an operating frequency between 250 and 300 kHz, and a resolution of 512 × 512. Optical images were taken with an Olympus BX51 Microscope equipped with an Olympus DP70 Microscope Digital Camera.

3. Results and discussions

Fig. 2A is a TEM image of the self-assembled monolayer film formed by copolymer **1** micelles from *p*-xylene. The spherical micelles formed films with well-ordered hexagonal close packed arrays. The dark regions are the PMPCS core, and the grey area between the spherical dark cores is the PS shell. Since the electron density of the PMPCS is larger than the PS, no staining is needed for TEM observations. The observed film was a single monolayer as no overlap of the particles was observed, which would indicate a multi-layer film. The center-to-center distance between the particles was, on average, 141 nm, with very small particle distribution of ±4 nm. Despite the slightly large polydispersity (PDI = 1.38) of copolymer **1**, the diameter distribution of spherical micelles after self-assembly is very narrow, with only 3% deviation, which agrees well with observations from laser light scattering results [38]. The micelle solution can easily form monolayer films larger than 100 µm^2 in area. The inset is the fast Fourier transform (FFT) image of the particle array. The spots indicate a very regular hexagonal packing of the spherical micelles in the film. These films have a continuous layer of micelles with no hole defects; however, there are several packing defects in the film. Using the method of

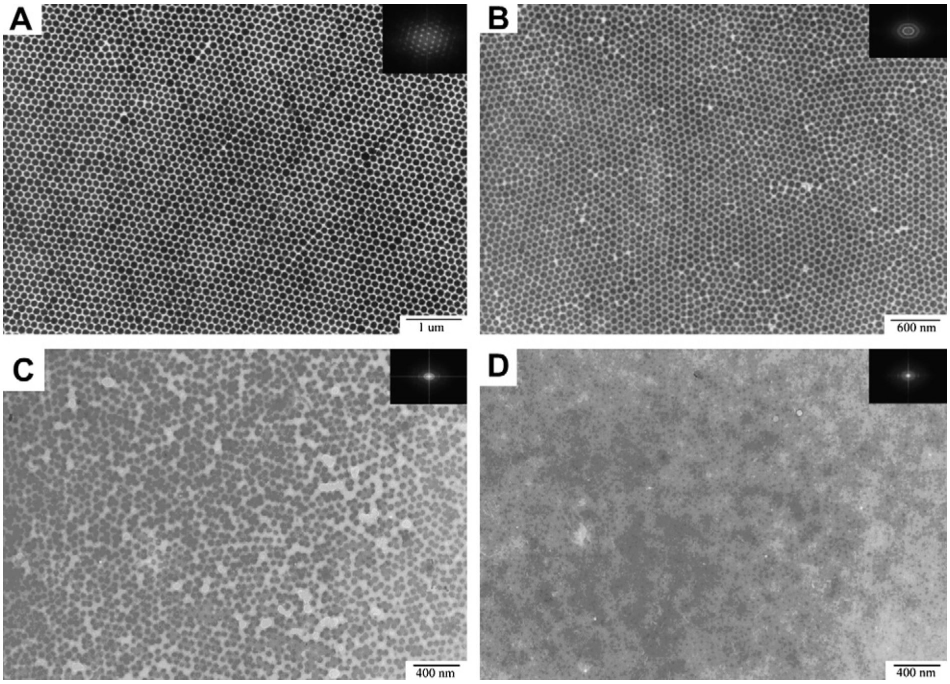

Fig. 2. TEM images of copolymer micelle monolayer films formed in *p*-xylene at a concentration of 2.0 mg/ml by copolymer **1** (A), copolymer **2** (B), copolymer **3** (C) and copolymer **4** (D). Inset at right top of each figure is the FFT of the obtained particle arrays.

Segalman et al. [41], there is about 1 dislocation defect per 10 μm^2 on average for the micelles in Fig. 2A.

To demonstrate control over micelle size, we prepared micelles of copolymers **2**, **3** and **4** at the same concentration by the same process as copolymer **1**. Fig. 2B–D shows the TEM images of the films formed by the corresponding block copolymers. In all of these films, the dark spheres are the PMPCS micelles cores. For block copolymer **2**, the micelles also formed a well-ordered hexagonal close packed film as seen in Fig. 2B. However, there are more defects in these films than in the films formed by copolymer **1**. The increased defect level with reduced micelle diameter is very clear. In the mono-layer film of copolymer **3**, as seen in Fig. 2C, the hexagonal close packing greatly diminishes with an even higher concentration of defects, including hole defects. The positional order was almost lost (see FFT inset). When the block length is reduced to that found in copolymer **4**, the spherical micelle arrangement is totally random as shown in Fig. 2D. The FFT images of each are included in the figure and support the lack of order with decreasing particle size.

There are many issues that can affect micelle film formation. In our case, the reason that the larger micelles formed a more ordered structure during film formation is possibly due to their larger size (which may make them inert to thermal fluctuations or vibrations) or the surface density of PS coils in micelle shell (where the repulsion/stabilization from the PS brushes between micelle shells is minimal because of the lower surface density). In the smaller micelles, the lack of these effects is more influential and results in poorer packing. Since all other parameters are identical in these different films, the micelle size and number of chains must be the origin of the differences in packing.

Fig. 2A–D indicates that the particle core size can be controlled by the PMPCS block copolymer length. For copolymer **1**, the average particle diameter is 140 nm. For copolymer **2**, the particle diameter

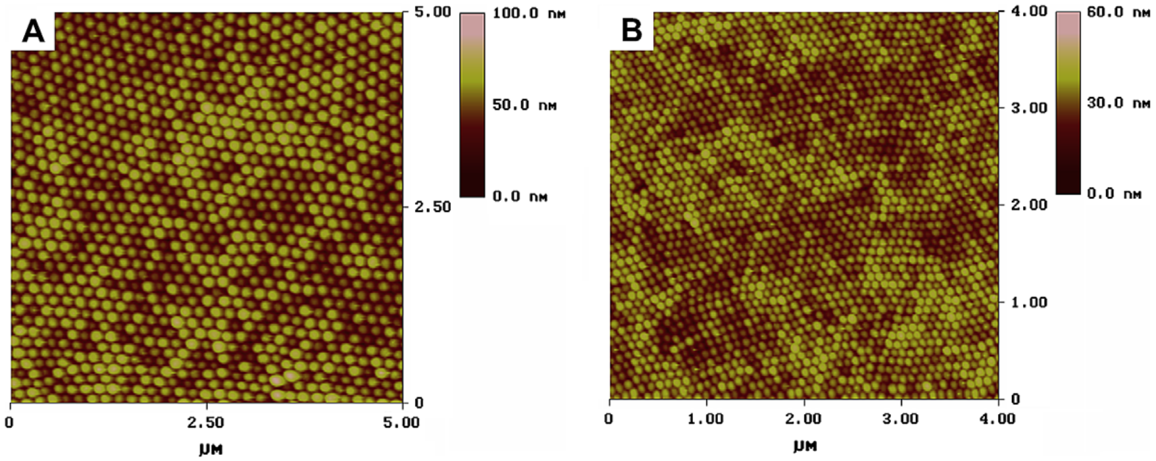

Fig. 3. AFM images of the monolayer film formed by copolymer **1** (A) and copolymer **2** (B) micelles from *p*-xylene with concentration of 2.0 mg/ml.

is about 85 nm with the PMPCS core size of about 68 nm. For copolymer **3** and copolymer **4**, the core diameters are on average 50 nm and 30 nm, respectively, while the distance between the particles cannot be calculated due to the poor packing. The LLS measurements in our previous work indicated a micelle diameter of 155 nm for copolymer **2**, 120 nm for copolymer **3** and 105 nm for copolymer **4** [39]. This size difference is partially accounted for by larger micelles contributing more to the LLS signal and by the particle size shrinking after the solvent evaporation during film formation. This means the PS coils in the micelles collapsed during the solvent evaporation process. The PMPCS core size coincides with the core size observed by the single micelle in TEM but is still slightly smaller than that calculated from the LLS in solution.

To further investigate how the micelles packed in the monolayer film, AFM was used to characterize the micelle films of copolymers **1** and **2**. AFM measurements show the particle diameter clearly. Fig. 3A shows an AFM image of the monolayer micelle film for copolymer **1**. In this film, well-ordered hexagonal close packed arrays of the spherical micelles were observed. The particle size obtained from AFM was 145 nm on average, agreeing well with the value obtained from TEM images. Fig. 3B is an AFM image of the micelle film from copolymer **2**, where a well-ordered hexagonal packing was also observed. The particle size from AFM was 90 nm on average, agreeing well with the data obtained from TEM images. These AFM images also show the surface topography, which cannot be observed in TEM.

Controlling the micelle morphology is an important issue in block copolymer self-assembly. We know that copolymer **2** can form worm-like (cylindrical) micelles at some specific concentrations ($c = 0.06$ mg/ml) in *p*-xylene. After the worm-like micelles were formed, the copolymer solution was deposited onto a water surface for the solvent to evaporate. Fig. 4 is a TEM image of the mono-layer film formed from worm-like micelles. In the worm-like micelles, the inner PMPCS rods appear dark in the TEM image and the surrounding PS shell appears grey between two adjacent worm-like micelles. The diameter of the cylindrical micelle is 80 nm on average, with the diameter of core rods being 60 nm, and the micelle length being several microns. Since the worm-like micelles have greater mobility constraints, one would expect poor packing in the worm-like micelles films. In Fig. 4, there is no significant orientation in the film, and the film contains a number of holes. The restricted mobility of the cylindrical micelles caused a lot of defects in the film. Interestingly, the end of the worm-like micelles is little bigger than the rest of the worm-like micelles and looks like a spherical micelle. This could give insight into how the inner PMPCS block is packed in the worm-like micelles and the mechanism for the transition between spherical and cylindrical micelles. For the PS-*b*-PMPCS copolymer in *p*-xylene system, we have not found the condition for preparing micelle solutions with only worm-like micelles. The worm-like micelles always coexist with a small portion of spherical micelles. To our knowledge, this is the first reported monolayer film formed by worm-like cylindrical micelles. If an external shearing force was applied during the film formation, we believe the packing of the worm-like micelles would improve.

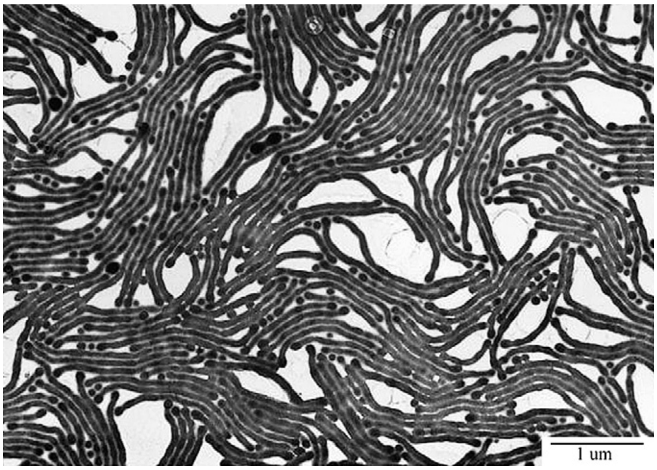

Fig. 4. TEM image of the monolayer film formed by cylindrical micelles. Film was formed by casting copolymer **2** solution at a concentration of 6.0×10^{-5} g/ml in *p*-xylene on the water surface.

The well-ordered hexagonal packing of the spherical micelles and the controlled diameter of the particle size by block copolymer length make this system very interesting. We observed that there are only a few point defects in the films for copolymers **1** and **2**. Besides opportunities for use as masks for lithography, this system has potential applications in photonic opals since the large spherical micelles are around 100 nm, which is appropriate for fabricating opal templates or to make photonic crystals, and the particle distribution is very narrow. Traditionally, examples of colloids in literature to fabricate opals are from inorganic silica colloids or polymer latexes [42–51]. Since opals need monodispersed colloids to be fabricated, which is not easy to be synthesized and only a few systems meet this requirement, the advantage to use polymer

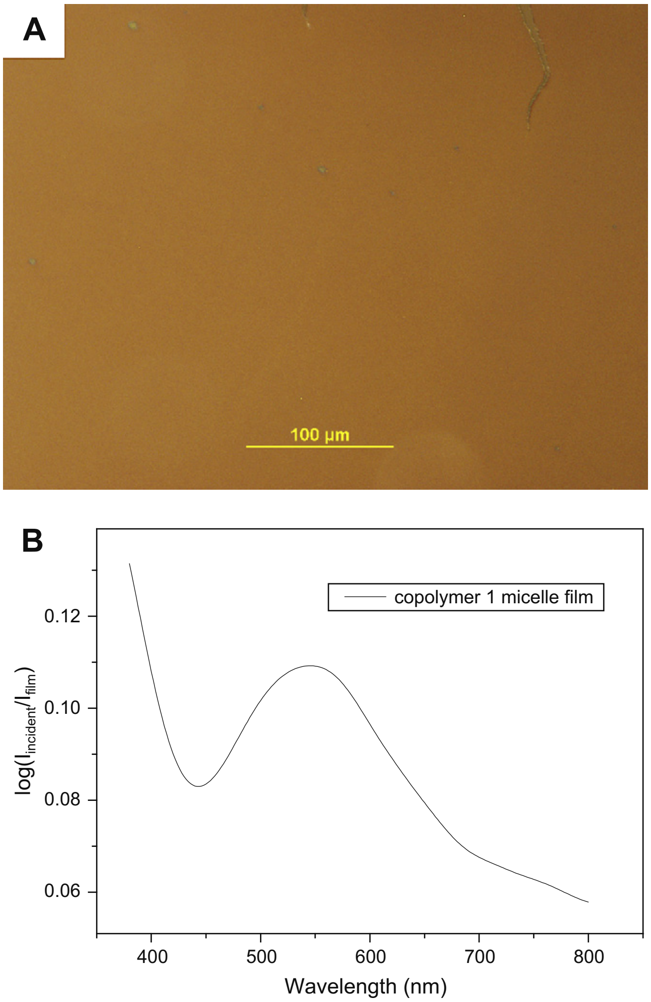

Fig. 5. Optical microscopy picture of the micelle film of copolymer **1** in reflection mode (A) and UV–Vis adsorption spectrum of a copolymer **1** micelle film (B).

micelles over traditional colloids derives from the tunable size and narrow size distribution. The size can be tuned by adjusting the molecular weight of the insoluble block, where the slightly large polydispersity of starting block copolymers can be tolerated, as they will form monodispersed micelles in the self-assembly process. Thus, they also fulfill the particle polydispersity requirement for photonic opals. This means a lot of block copolymers, synthesized by controlled polymerization with narrow polydispersity, can be used as templates. As far as we know, there are no publications concerning the use of well-organized micelle films to fabricate opals, and our system may open a new route to fabricate opal or reverse opal crystals.

The monolayer micelle films were analyzed for their optical characteristics. The PS-*b*-PMPCS block copolymers do not have an absorption band in the visible light wavelength region and appear transparent under optical microscopy for bulk films. Fig. 5A is the optical microscopy picture of the monolayer micelle film of copolymer **1** in reflection mode. The film size exceeds 10,000 μm^2 with very few hole defects, making large area films for photonic crystal fabrication possible. The film appeared red in reflection mode. This color is due to the reflection band caused by coherent backscattering from the block copolymer micelle array with 2D hexagonal packing. Fig. 5B is the absorption spectrum from the film measured by UV–Vis spectroscopy. The spectrum shows an absorption peak from 460 nm to 630 nm with a maximum absorption at 545 nm (green light region). Since red is the complement of green, the film appeared red in reflection optical microscopy. For comparison, block copolymer films prepared from copolymers **3** and **4** did not show any color in optical microscopy, mostly due to their poor packing. The optical applications of well-ordered films prepared from block copolymer micelles are currently under investigation.

4. Conclusions

PS-*b*-PMPCS copolymers formed spherical core-shell micelles in *p*-xylene that can be assembled into a monolayer film. Well-ordered hexagonal close packed arrays were observed with micelles prepared from copolymers **1** and **2**, as observed by TEM and AFM. The core-shell structure of the micelles was maintained in the film with little shrinkage of the core size and significant shrinkage of the outside solvated PS shell after solvent evaporation. Since the micelle size can be controlled by the block copolymer length, films can be formed from micelles of different sizes. Worm-like micelles were also used to fabricate a mono-layer film. The cylindrical micelles did not pack well. They do not have any orientation in the film, and there are significant holes. The well-ordered micelle films from copolymer **1** have a reflection absorption peak centered at 545 nm as the result of the regularly-packed micelles in the film.

Acknowledgment

We are grateful to the National Natural Science Foundation of China (Grants 20674001, 20134010, 20634010 and 20574002), the National Distinguished Young Scholar Fund of China (Grant 20325415) and the National Science Foundation of US (DMR-0906898).

References

[1] Bates FS, Fredrickson GH. Annu Rev Phys Chem 1990;41:525–57.
[2] Hamley IW. The physics of block copolymers. Oxford: Oxford University; 1998.
[3] Park C, Yoon J, Thomas EL. Polymer 2003;44:6725–60.
[4] Li M, Ober CK. Mater Today 2006;9:30–9.
[5] Eloi J-C, Chabanne L, Whittell GR, Manners I. Mater Today 2008;11:28–36.
[6] Kim G, Libera M. Macromolecules 1998;31:2569–77.
[7] Niu S, Saraf RF. Macromolecules 2003;36:2428–40.
[8] Xu T, Goldbach JT, Misner MJ, Kim S, Gibaud A, Gang O, et al. Macromolecules 2004;37:2972–7.
[9] Harant AW, Bowman CN. J Vac Sci Technol B 2005;23:1615–21.
[10] Tang C, Bang J, Stein GE, Fredrickson GH, Hawker CJ, Kramer EJ, et al. Macromolecules 2008;41:4328–39.
[11] Park S, Kim B, Xu J, Hofmann T, Ocko BM, Russell TP. Macromolecules 2009;42:1278–84.
[12] Alexandris P, Lindman B. Amphiphilic block copolymers: self-assembly and applications. Amsterdam: Elsevier; 2000.
[13] Zhang L, Eisenberg A. J Am Chem Soc 1996;118:3168–81.
[14] Jenekhe SA, Chen XL. Science 1998;279:1903–7.
[15] Zubarev ER, Pralle MU, Li L, Stupp SI. Science 1999;283:523–6.
[16] Klok HA, Langenwalter JF, Lecommandous S. Macromolecules 2000;33:7819–26.
[17] Wu J, Pearce EM, Kwei KT, Lefebvre AA, Balsara NP. Macromolecules 2002;35:1791–6.
[18] Jain S, Bates FS. Science 2003;300:460–4.
[19] Bhargava P, Tu Y, Zheng JX, Quirk RP, Li P, Harris FW, et al. Macromolecules 2006;39:4880–8.
[20] Bhargava P, Tu Y, Zheng JX, Xiong H, Quirk RP, Cheng SZD. J Am Chem Soc 2007;129:1113–21.
[21] Sukhorukov GB, Susha AS, Davis S, Leporatti S, Donath E, Hartmann J, et al. J Colloid Inter Sci 2002;247:251–4.
[22] Nguyen PM, Zacharia N, Verploegen SE, Hammond PT. Chem Mater 2007;19:5524–30.
[23] Förster S, Antonietti M. Adv Mater 1998;10:195–217.
[24] Spatz J, Möβmer S, Möller M, Kocher M, Neher D, Wegner G. Adv Mater 1998;10:473.
[25] Spatz JP, Mössmer S, Hartmann C, Möller M. Langmuir 2000;16:407–15.
[26] Webber GB, Wanless EJ, Butun V, Armes SP, Biggs S. Nano Lett 2002;2:1307–13.
[27] Glass R, Möller M, Spatz JP. Nanotechnology 2003;14:1153–60.
[28] Hamley IW. Angew Chem Int Ed 2003;42:1692–712.
[29] Soulantica K, Maisonnat A, Fromen M-C, Casanove M-J, Chaudret B. Angew Chem Int Ed 2003;42:1945–9.
[30] Feyter SD, Abdel-Mottaleb MMS, Schuurmans N, Verkuijl BJV, Esch JHV, Feringa BL, et al. Chem Eur J 2004;10:1124–32.
[31] Yoo SI, Sohn B-H, Zin W-C, Jung JC. Langmuir 2004;20:10734–6.
[32] Dai C-A, Wu Y-L, Lee Y-H, Chang C-J, Su W-F. J Cryst Growth 2006;288:128–36.
[33] Aizawa M, Buriak JM. J Am Chem Soc 2006;128:5877–86.
[34] Kronholz S, Rathgeber S, Karthäuser S, Kohlstedt H, Clemens S, Schneller T. Adv Funct Mater 2006;16:2346–54.
[35] Lu J, Kopley T, Dutton D, Liu J, Qian C, Son H, et al. J Phys Chem B 2006;110:10585–9.
[36] Tung P-H, Kuo S-W, Jeong K-U, Cheng SZD, Huang C-F, Chang F-C. Macromol Rapid Commun 2007;28:271–5.
[37] Marencic AP, Wu MW, Register RA. Macromolecules 2007;40:7299–305.
[38] Tu Y, Wan X, Zhang D, Zhou Q-F, Wu C. J Am Chem Soc 2000;122:10201–5.
[39] Tu Y, Wan X, Zhang H, Fan X, Chen X, Zhou Q-F, et al. Macromolecules 2003;36:6565–9.
[40] Wan X, Tu Y, Zhang D, Zhou Q-F. Polym Int 2000;49:243–7.
[41] Segalman RA, Hexemer A, Hayward RC, Kramer EJ. Macromolecules 2003;36:3272–88.
[42] Asher SA, Holtz J, Liu L, Wu Z. J Am Chem Soc 1994;116:4997–8.
[43] Wijnhoven JEGJ, Vos WL. Science 1998;281:802–4.
[44] Busch K, John S. Phys Rev E 1998;58:3896–908.
[45] Johnson SA, Ollivier PJ, Mallouk TE. Science 1999;283:963–5.
[46] Jiang P, Cizeron J, Bertone JF, Colvin VL. J Am Chem Soc 1999;121:7957–8.
[47] Ramos L, Lubensky TC, Dan N, Nelson P, Weitz DA. Science 1999;286:2325–8.
[48] Xia Y, Gates B, Yin Y, Lu Y. Adv Mater 2000;12:693–713.
[49] Edrington AC, Urbas AM, DeRege P, Chen CX, Swager TM, Hadjichristidis N, et al. Adv Mater 2001;13:421–5.
[50] Ozaki R, Matsui T, Ozaki M, Yoshino K. Appl Phys Lett 2003;82:3593–5.
[51] Yoon J, Lee W, Thomas EL. Macromolecules 2008;41:4582–4.